Immunoproteasome Inhibition

DOI: 10.1002/anie.201406964

Selective Inhibition of the Immunoproteasome by Ligand-Induced Crosslinking of the Active Site **

Christian Dubiella, Haissi Cui, Malte Gersch, Arwin J. Brouwer, Stephan A. Sieber, Achim Krüger, Rob M. J. Liskamp, and Michael Groll**

Abstract: *The concept of proteasome inhibition ranks among the latest achievements in the treatment of blood cancer and represents a promising strategy for modulating autoimmune diseases. In this study, we describe peptidic sulfonyl fluoride inhibitors that selectively block the catalytic β5 subunit of the immunoproteasome by inducing only marginal cytotoxic effects. Structural and mass spectrometric analyses revealed a novel reaction mechanism involving polarity inversion and irreversible crosslinking of the proteasomal active site. We thus identified the sulfonyl fluoride headgroup for the development and optimization of immunoproteasome selective compounds and their possible application in autoimmune disorders.*

The 20S proteasome (core particle; CP) is a sensitive target for the clinically applied inhibitors bortezomib (Velcade) and carfilzomib (CFZ, Kyprolis; Figure 1). Its blockage in malignant cells emerged as an effective approach for the treatment of blood cancers such as multiple myeloma and mantle cell lymphoma.[1,2] Moreover, the ongoing evaluation of the anti-inflammatory immunoproteasome (iCP) inhibitor ONX 0914 (former PR-957; Figure 1) in preclinical studies has givenrise to a novel therapeutic strategy for modulating autoimmune disorders including rheumatoid arthritis and multiple sclerosis.[3,4] A special attribute of ONX 0914 is the reduction of disease-associated immune responses by selectively blocking the β5 subunit of the iCP (β5i or LMP7).[3] However, the therapeutic window of iCP inhibitors like ONX 0914 entirely depends on their selectivity for β5i over β5c, in order to prevent cytotoxic effects that arise from undesired co-

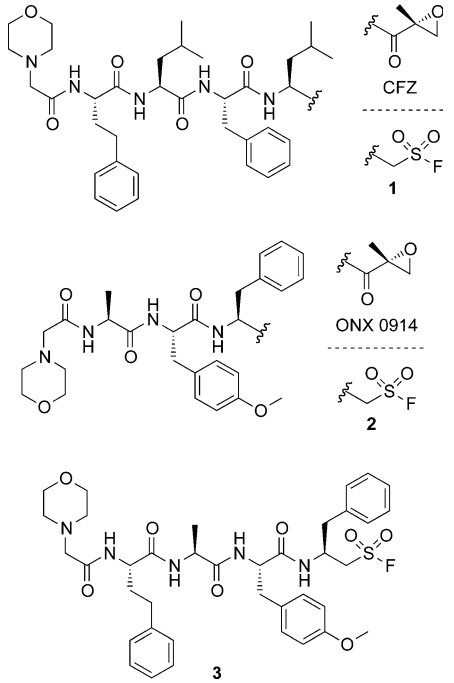

Figure 1. α′,β′-Epoxyketones carfilzomib (CFZ) and ONX 0914 as well as their peptido sulfonyl fluoride (PSF) counterparts **1**, **2**, and compound **3**.

inhibition of the constitutive proteasome (cCP).[5,6] Thus, the decisive element of iCP inhibitor design is the capability to discriminate between the similar chymotrypsin-like (ChTL) activities of β5i and β5c.[7] CFZ as well as ONX 0914 feature an electrophilic α′,β′-epoxyketone warhead that forms a covalent and irreversible adduct with both nucleophiles, Thr1O$^{\gamma}$ and Thr1N, of the catalytically active threonine (Thr1) at the β5 subunit (see Scheme S1 in the Supporting Information).[8–10] Since CFZ and ONX 0914 have identical warheads, ONX 0914's favorable binding to β5i solely originates from its backbone architecture, which fulfills the individual binding requirements of β5i as opposed to β5c.[11] Recently, extensive research on the optimization of peptide backbones by incorporation of unnatural amino acids resulted in β5i- and β5c-specific epoxyketones.[5,12,13] However, studies on various functional reactive groups and peptido sulfonyl fluoride (PSF) proteasome inhibitors suggest that also warheads have a direct influence on the selectivity for individual active β-subunits.[14–16] Notably, PSF compounds block the CP activity in the low nanomolar range,[16] albeit they are the only peptidic CP inhibitors known so far whose electrophilic

[*] C. Dubiella, Dr. M. Gersch, Prof. Dr. S. A. Sieber, Prof. Dr. M. Groll
Center for Integrated Protein Science Munich (CIPSM)
Department of Chemistry, Technische Universität München
Lichtenbergstrasse 4, 85747 Garching (Germany)
E-mail: michael.groll@tum.de
Prof. Dr. R. M. J. Liskamp
University of Glasgow
University Avenue, Glasgow G12 8QQ (UK)
E-mail: robert.liskamp@glasgow.ac.uk
H. Cui, Prof. Dr. A. Krüger
Institute for Experimental Oncology and Therapy Research
Technische Universität München, 81675 München (Germany)
A. J. Brouwer
Utrecht University, 3508 TB Utrecht (The Netherlands)

[**] This work was funded by SFB 1035A2 and DFG GR 1861/10-1. We thank R. Feicht, R. Baur, and A. Späth for assistance with the experiments and the staff of PXI of Paul Scherrer Institute, Swiss Light Source (Villigen, Switzerland) for help with data collection.

Supporting information for this article is available on the WWW under http://dx.doi.org/10.1002/anie.201406964.

headgroup is shifted by a methylene unit, which demands an exceptional binding mode. Therefore, we set out to elucidate the PSF's mode of action, commencing with the synthesis of the CFZ and ONX 0914 PSF counterparts **1** and **2** (Figure 1). Next, we determined crystal structures of yeast CP (yCP):**1** with resolutions up to 2.1 Å by performing crystal soaking experiments with incubation times of 1–6 h prior to data collection (see Table ST1).

Based on the identical headgroups of the PSF and the common serine protease inhibitor phenylmethanesulfonyl fluoride (PMSF), we anticipated a similar inactivation mechanism through the formation of a covalent adduct on Thr1 upon attack of Thr1O$^{\gamma}$ on the sulfur atom. Unexpectedly, after incubation of the crystal for 2 h, the yCP:**1** structure revealed empty substrate binding channels (2.1 Å resolution, $R_{free} = 19.7\,\%$, PDB ID 4R17). Instead, the $F_o - F_c$ map displayed negative electron density at the Thr1 side chain of subunit β5, disclosing a chemical modification of the catalytic center (see Figure S1a), whereas β1 and β2 remained identical to the apo state. To identify a short-lived reaction intermediate of **1** at β5 we conducted time-resolved intact protein mass spectrometry using LC-ESI-LTQ-FT-MS analysis on various CP types incubated with **1** and **2** (Figure 2).

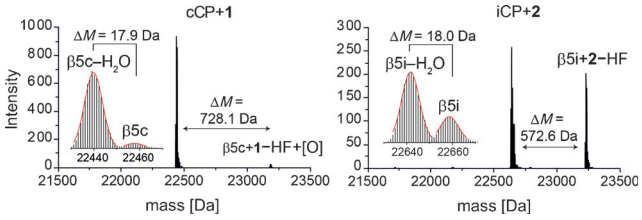

Figure 2. Deconvoluted intact-protein mass spectra of the β5c and β5i subunits following treatment of cCP with **1** (left panel) and iCP with **2** (right panel) (25 μM) after incubation for 12 h. The species labeled "$-H_2O$" represent either the aziridine or the crosslinked state (expected mass difference: 18.0 Da). The insets feature enlargements of the major species. The species labeled "+**2**−HF" represents the covalently modified intermediate of the β5 subunits prior to dehydroxylation (expected mass difference: 572.7 Da). See Figure S5 for spectra of β5 of untreated cCP and iCP.

Spectra with incubation times up to 2 h confirmed the formation of a covalent adduct on the β5 subunit of all applied CP types with an observed mass increase corresponding to the ligand upon fluorine release (see Figure 2 and Figure S2). Furthermore, we observed a formal loss of a water molecule (−18 Da) at the β5 subunit which was validated by multiple experiments and different mass spectra deconvolution algorithms (see Figures S3 and S4 and Tables ST2 and ST3).

These findings suggest either an addition–elimination reaction as described for PMSF, which for example converts the active Ser195 of thrombin into dehydroalanine,[17] or an addition–displacement mechanism comprising sulfonylation of Thr1O$^{\gamma}$, followed by an intramolecular substitution by Thr1N to yield an aziridine. While the PMSF-induced elimination reaction requires strong alkaline conditions, our experiments were carried out at pH 6.8–7.5, indicating that dehydroxylation of Thr1 is rather an integral part of the inhibition mechanism than an artificially base-induced event. Consistently, the $F_o - F_c$ electron density map clearly depicts the intramolecular displacement product (*S*,*S*)-aziridine-T1′ (Figure 3b), thus excluding the elimination product (*E*)-dehydrobutyrine (Dhb) (Figure S1b, Supporting Information). Moreover, cyclization initiated by Thr1N is confirmed

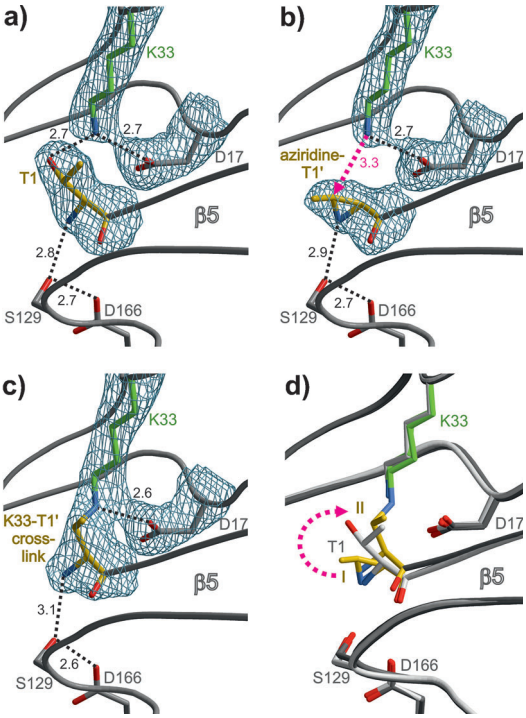

Figure 3. Comparative X-ray analysis of the β5 active site after time-dependent soaking experiments of yCP crystals with **1**. The $2F_o - F_c$ electron density maps (blue mesh, contoured at 1σ) show distances in Å as black dashed lines. The active site triad Thr1 (T1), Asp17 (D17), and Lys33 (K33) has been excluded prior to phasing. Stereoviews of (a)–(d) are depicted in Figure S6. a) Subunit β5 of the apo structure with unmodified T1 (yellow).[18] b) Aziridine-T1′ (yellow) formation on β5 after 2 h soaking time with **1**. The trajectory of the nucleophilic attack of K33 (green) is shown as a pink dashed arrow (PDB ID 4R17). c) K33-T1′-crosslink (yellow) formation on subunit β5 after 6 h soaking time (PDB ID 4R18). d) Superposition of the apo structure with unmodified T1 (light gray), the aziridine-T1′ intermediate (I, yellow), and the K33-T1′-crosslink (II, yellow). The structural rearrangement of T1 upon its conversion into intermediate I and crosslink II is illustrated with a pink dashed arrow.

by the inverted stereoconfiguration of the methyl group in (*S*,*S*)-aziridine-Thr1′, implying an S_N2-like displacement. To analyze the stability of the aziridine ring we conducted further soaking experiments with extended incubation times up to 6 h at pH 6.8. The $2F_o - F_c$ electron density map of the yCP:**1** structure revealed a S_N2-type ring-opening of the aziridine-Thr1′ by attack of the amino group of Lys33 (Lys33N$^{\varepsilon}$), yielding an intramolecular crosslink in β5 (Figure 3c; 2.4 Å resolution, $R_{free} = 19.5\,\%$, PDB ID 4R18). This Lys33-Thr1′ bond proves the presence of a polarity-inversed Thr1 intermediate and is certainly surprising, since the function of Lys33N$^{\varepsilon}$ is to maintain the pK_a of Thr1O$^{\gamma}$, and hence

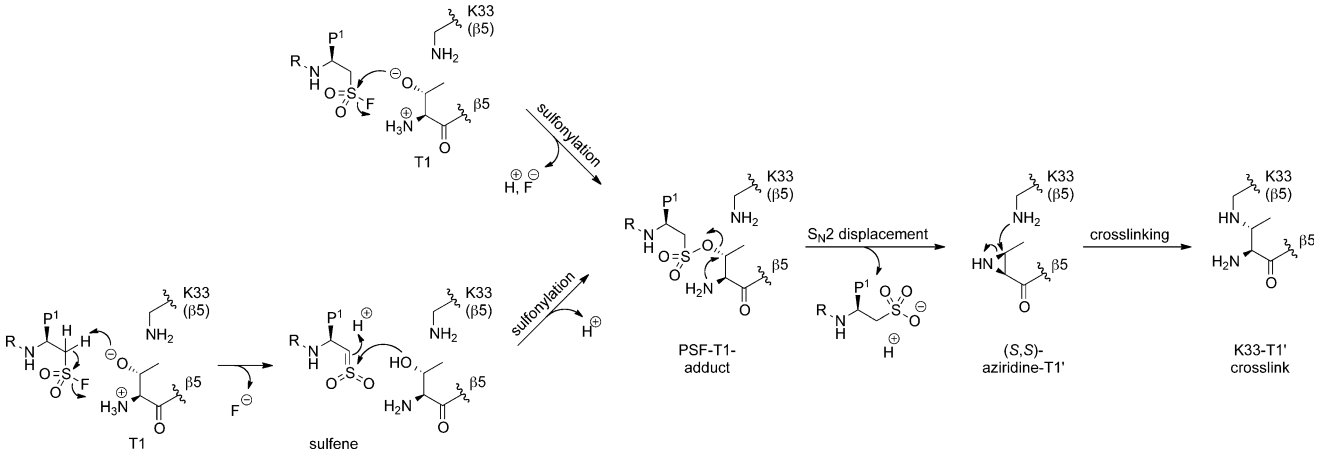

Scheme 1. Proposed three-step inactivation mechanism of the PSF compounds at the proteasomal active site of subunit β5. Hypothetically, the sulfonylation of Thr1O$^{\gamma}$ is conceivable by two different mechanisms: a direct nucleophilic attack of Thr1O$^{\gamma}$ on the electrophilic sulfur center (upper left corner), or by elimination and sulfene formation (lower left corner). The substituent R indicates the rest of the peptidic backbone and P^{1} refers to the amino acid side chain of the inhibitor protruding into the S1 specificity pocket.

possesses only a moderate intrinsic nucleophilicity.[19] From an organic chemical point of view this aziridine ring-opening is also unexpected, since normally the presence of electron-withdrawing groups on the aziridine nitrogen is required.[20]

Intriguingly, superposition of the apo and yCP:**1** structures illustrates that the flexibility of the aziridine-Thr1′-containing β5 chain solely accounts for closing the 3.3 Å gap between Lys33N$^{\varepsilon}$ and the electrophile, while all remaining residues retain their position (Figure 3d). Consequently, the decline of structural integrity upon dehydroxylation of Thr1 presents a precondition to perform the crosslinkage. Based on these distinct snapshots of the reaction intermediates, we propose a three-step mechanism of the PSF compounds resulting in the crosslinking of the proteasomal active site (Scheme 1).

Our next goal was to investigate whether this complex mechanism could contribute to increased β5i selectivity and thus reduced cytotoxicity. Therefore, we compared the potency and β5 subunit selectivity of **1** and **2** with that of their α′,β′-epoxyketone originals by performing in vitro IC$_{50}$ assays with purified human iCP, cCP, and yeast CP (yCP) (Table 1, Figure 4). Remarkably, **2** (IC$_{50}$ β5c/β5i: 25) turned out to be roughly three times more selective for β5i than ONX 0914 (IC$_{50}$ β5c/β5i: 9), despite identical backbone architecture. However, the improved β5i selectivity of **2** was accompanied by a 20-fold decreased potency (IC$_{50}$ (β5i): 1134 nM) compared to ONX 0914 (IC$_{50}$ (β5i): 57 nM), indicating that PSF ligands require at least capped tetrapeptidic backbones for sufficient stabilization during proteasomal binding. Thus, we extended **2** with a homophenylalanine in P4 to generate compound **3** (Figure 1).

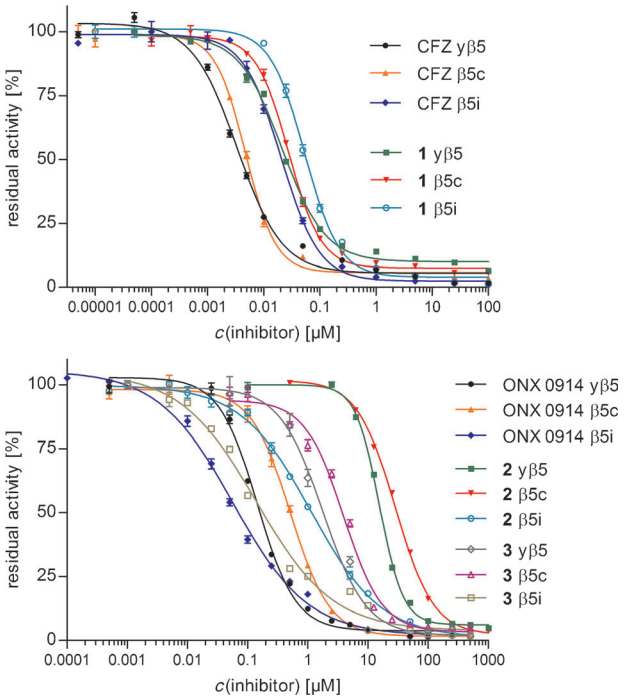

Figure 4. In vitro IC$_{50}$ assays against the ChTL activity of various purified CP types after 1 h incubation at various concentrations of CFZ and **1** (left panel) as well as ONX 0914, **2**, and **3** (right panel) using a fluorogenic substrate assay. Data of three repetitions were normalized to DMSO-treated controls and are presented as relative activity with standard deviation (Table 1).

Table 1: In vitro IC$_{50}$ values [nM] against the ChTL activity of various purified CP types.

Compound	IC$_{50}$ yβ5	IC$_{50}$ β5c	IC$_{50}$ β5i	IC$_{50}$ β5c/β5i[a]
CFZ	3 ± 1	5 ± 1	21 ± 3	0.2
1	21 ± 2	28 ± 2	54 ± 10	0.5
ONX 0914	145 ± 15	513 ± 30	57 ± 10	9
2	15420 ± 635	28460 ± 1305	1134 ± 146	25
3	1775 ± 476	3927 ± 550	139 ± 34	28

[a] A high IC$_{50}$ β5c/β5i ratio indicates selectivity for β5i.

Since the S4 specificity pockets of iCP and cCP are identically shaped by the β6 subunit, **3** exhibited up to eightfold improved potency against β5i (IC$_{50}$ (β5i): 139 nM) and β5c (IC$_{50}$ (β5c): 3927 nM), respectively. Importantly, **3**

Table 2: In vivo IC_{50} values [nM] against the ChTL activity and LC_{50} values [nM] against HeLa and THP-1 cells.

Compound	IC_{50} HeLa	IC_{50} THP-1	LC_{50} HeLa	LC_{50} THP-1	LC_{50}/IC_{50}[a] HeLa	LC_{50}/IC_{50}[a] THP-1
CFZ	6±1	7±1	28±6	12±1	5	2
1	29±3	35±4	353±63	156±16	12	4
ONX 0914	78±10	22±2	333±48	110±14	4	5
2	5032±577	1789±378	>100000	>100000	>19	>56
3	550±59	146±40	>100000	5746±1436	>182	39

[a] A high LC_{50}/IC_{50} ratio indicates low cytotoxicity relative to the corresponding IC_{50} value.

displayed an even enhanced β5i selectivity (IC_{50} β5c/β5i: 28) compared to **2**. By contrast, **1** and CFZ inhibited the β5 subunits of all analyzed CP types in the single- and double-digit nanomolar range without any preference for β5i. This suggests that the PSF headgroup emphasizes the influence of the peptidic backbone to a greater extent than the α′,β′-epoxyketone warhead.

The in vitro findings were confirmed by determining the in vivo IC_{50} values of **1**, **2**, their α′,β′-epoxyketone counterparts as well as **3** in cell culture assays (Table 2, Figure 5a). We used either the THP-1 cell line, which is derived from acute monocytic leukemia and expresses high levels of iCP, or the HeLa cell line, which primarily contains cCP.[21] ONX 0914, **2**, and **3** turned out to be three to four times more selective for THP-1 cells over HeLa cells, while **1** and CFZ displayed virtually similar potencies on both cell lines in accordance with the in vitro IC_{50} assays.

To evaluate the cytotoxic profiles of the compounds we determined the LC_{50} values against THP-1 and HeLa cells in viability assays (Table 2, Figure 5b). Notably, **2** and **3** hardly affected the viability of either cell line, arguably reflecting their high β5i selectivity and low off-target binding. The in vivo IC_{50} values of **1** (IC_{50} (THP-1): 35 nM, IC_{50} (HeLa): 29 nM) exclude that the low cytotoxicity is caused by a rapid hydrolysis of the PSF headgroup.

In summary, the presented comparative study of iCP-selective α′,β′-epoxyketone and PSF counterparts highlights the sulfonyl fluoride headgroup as a promising motif for β5i targeting. In contrast to all analyzed CP inhibitors to date, PSFs manipulate the proteasomal activity by a previously unobserved mode of action through polarity inversion and intramolecular crosslinking of the active site. In contrast to the unspecific serine protease inhibitor PMSF, the additional peptidic backbone accounts for site-selective proteasome inhibition. Thus, target-specific iCP blockage of the PSF in the nanomolar range along with low cytotoxicity broadens the therapeutic window of PSF as potential future anti-inflammatory inhibitors.

Received: July 7, 2014
Published online: September 22, 2014

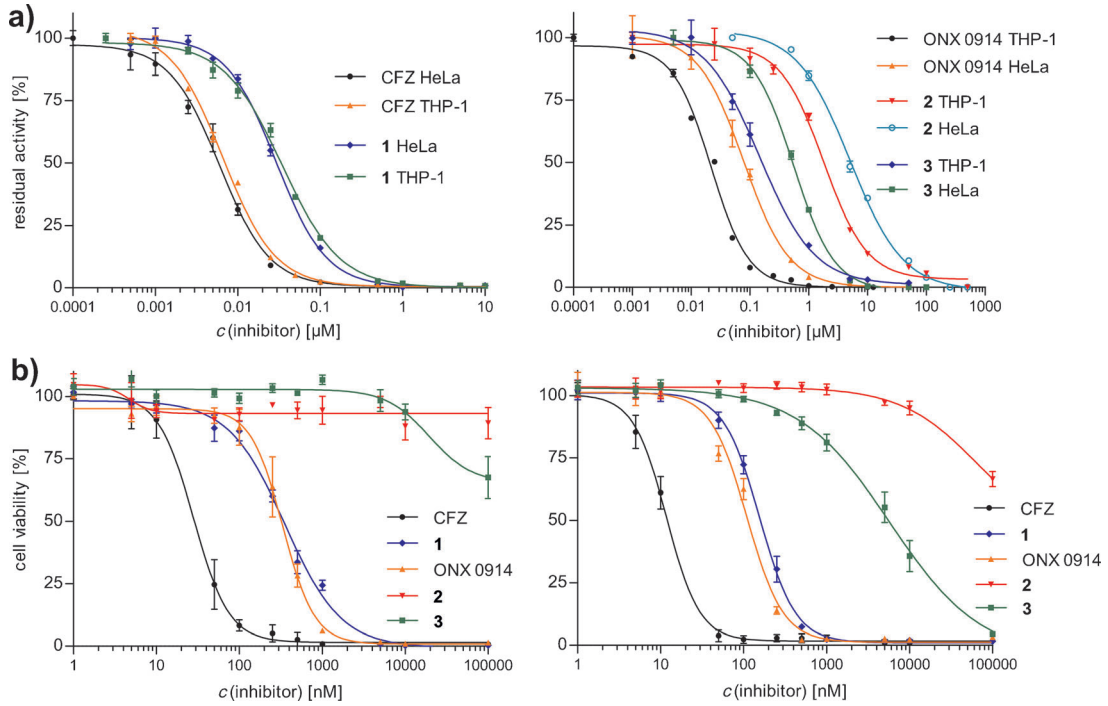

Figure 5. a) In vivo IC_{50} assays against the ChTL activity in HeLa and THP-1 cells after 105 min incubation at various concentrations of CFZ and **1** (left panel) as well as ONX 0914, **2**, and **3** (right panel) using a luminogenic substrate assay. b) LC_{50} against HeLa (left panel) and THP-1 (right panel) cells after 48 h incubation at concentrations of CFZ, **1**, ONX 0914, **2**, and **3** between 1 nM and 100 μM using an AlamarBlue-based cell viability assay. Data of three repetitions were normalized to DMSO-treated controls and are presented as relative activity with standard deviation (Table 2).

Keywords: drug design · inhibitors · immunoproteasome · peptido sulfonyl fluoride · umpolung

[1] P. G. Richardson, T. Hideshima, K. C. Anderson, *Cancer Control* **2003**, *10*, 361 – 369.
[2] S. D. Demo, C. J. Kirk, M. A. Aujay, T. J. Buchholz, M. Dajee, M. N. Ho, J. Jiang, G. J. Laidig, E. R. Lewis, F. Parlati, et al., *Cancer Res.* **2007**, *67*, 6383 – 6391.
[3] T. Muchamuel, M. Basler, M. A. Aujay, E. Suzuki, K. W. Kalim, C. Lauer, C. Sylvain, E. R. Ring, J. Shields, J. Jiang, et al., *Nat. Med.* **2009**, *15*, 781 – 787.
[4] M. Basler, S. Mundt, T. Muchamuel, C. Moll, J. Jiang, M. Groettrup, C. J. Kirk, *EMBO Mol. Med.* **2014**, *6*, 226 – 238.
[5] F. Parlati, S. J. Lee, M. Aujay, E. Suzuki, K. Levitsky, J. B. Lorens, D. R. Micklem, P. Ruurs, C. Sylvain, Y. Lu, et al., *Blood* **2009**, *114*, 3439 – 3447.
[6] D. Niewerth, J. van Meerloo, G. Jansen, Y. G. Assaraf, T. C. Hendrickx, C. J. Kirk, J. L. Anderl, S. Zweegman, G. J. L. Kaspers, J. Cloos, *Biochem. Pharmacol.* **2014**, *89*, 43 – 51.
[7] E. M. Huber, M. Groll, *Angew. Chem. Int. Ed.* **2012**, *51*, 8708 – 8720; *Angew. Chem.* **2012**, *124*, 8838 – 8850.
[8] M. Groll, K. B. Kim, N. Kairies, R. Huber, C. M. Crews, *J. Am. Chem. Soc.* **2000**, *122*, 1237 – 1238.
[9] L. Meng, R. Mohan, B. H. Kwok, M. Elofsson, N. Sin, C. M. Crews, *Proc. Natl. Acad. Sci. USA* **1999**, *96*, 10403 – 10408.
[10] A. Rentsch, D. Landsberg, T. Brodmann, L. Bülow, A.-K. Girbig, M. Kalesse, *Angew. Chem. Int. Ed.* **2013**, *52*, 5450 – 5488; *Angew. Chem.* **2013**, *125*, 5560 – 5599.
[11] E. M. Huber, M. Basler, R. Schwab, W. Heinemeyer, C. J. Kirk, M. Groettrup, M. Groll, *Cell* **2012**, *148*, 727 – 738.
[12] G. de Bruin, E. M. Huber, B.-T. Xin, E. J. van Rooden, K. Al-Ayed, K.-B. Kim, A. F. Kisselev, C. Driessen, M. van der Stelt, G. A. van der Marel, et al., *J. Med. Chem.* **2014**, *57*, 6197 – 6209.
[13] A. V. Singh, M. Bandi, M. A. Aujay, C. J. Kirk, D. E. Hark, N. Raje, D. Chauhan, K. C. Anderson, *Br. J. Haematol.* **2011**, *152*, 155 – 163.
[14] M. L. Stein, H. Cui, P. Beck, C. Dubiella, C. Voss, A. Krüger, M. Groll, *Angew. Chem. Int. Ed.* **2014**, *53*, 1679 – 1683; *Angew. Chem.* **2014**, *126*, 1705 – 1709.
[15] M. Screen, M. Britton, S. L. Downey, M. Verdoes, M. J. Voges, A. E. M. Blom, P. P. Geurink, M. D. P. Risseeuw, B. I. Florea, W. A. van der Linden, et al., *J. Biol. Chem.* **2010**, *285*, 40125 – 40134.
[16] A. J. Brouwer, A. Jonker, P. Werkhoven, E. Kuo, N. Li, N. Gallastegui, J. Kemmink, B. I. Florea, M. Groll, H. S. Overkleeft, et al., *J. Med. Chem.* **2012**, *55*, 10995 – 11003.
[17] R. W. Ashton, H. A. Scheraga, *Biochemistry* **1995**, *34*, 6454 – 6463.
[18] M. Groll, L. Ditzel, J. Löwe, D. Stock, M. Bochtler, H. Bartunik, R. Huber, *Nature* **1997**, *386*, 463 – 471.
[19] M. Groll, T. Clausen, *Curr. Opin. Struct. Biol.* **2003**, *13*, 665 – 673.
[20] X. E. Hu, *Tetrahedron* **2004**, *60*, 2701 – 2743.
[21] D. Niewerth, G. J. L. Kaspers, Y. G. Assaraf, J. van Meerloo, C. J. Kirk, J. Anderl, J. L. Blank, P. M. van de Ven, S. Zweegman, G. Jansen, et al., *J. Hematol. Oncol.* **2014**, *7*, 7.

